Supporting Information

Salvi et al. 10.1073/pnas.1501453112

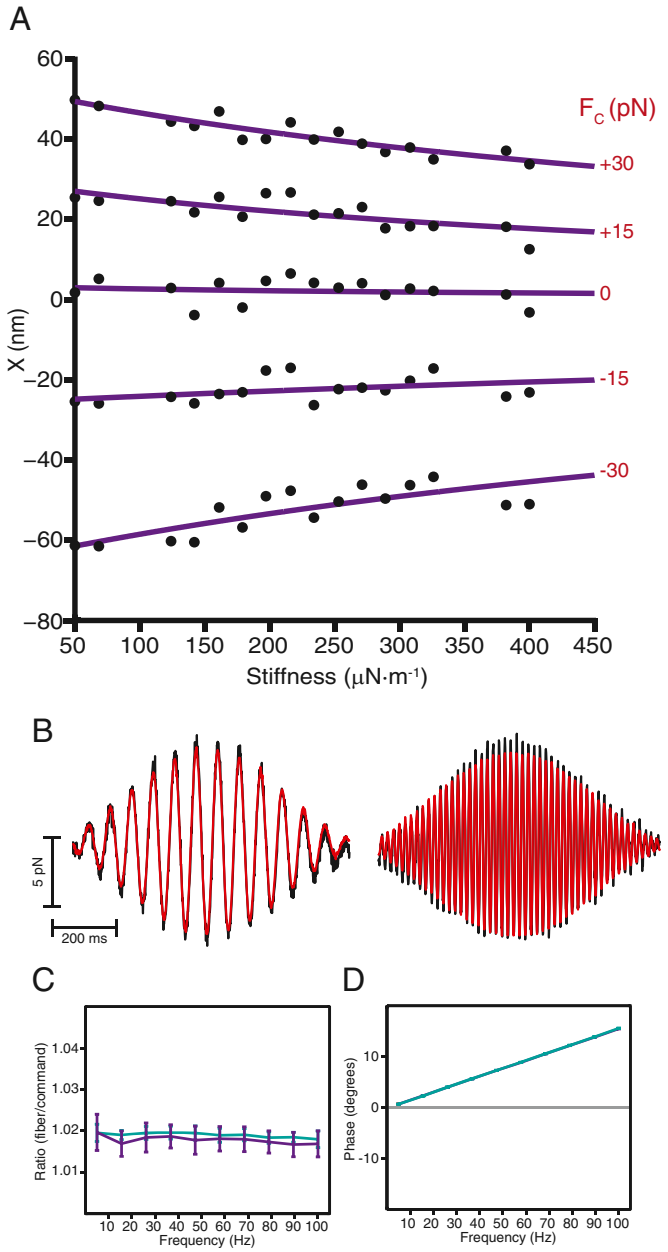

Fig. S1. Verification of the mechanical-load clamp. (*A*) To verify that the clamp allowed for simultaneous control of the load stiffness and constant force, we used a stimulus fiber of stiffness K_{SF} = 350 μN·m^{-1} and damping coefficient ξ_{SF} = 164 nN·s·m^{-1} to deliver force steps to a vertically mounted glass fiber of stiffness K_{HB} = 560 μN·m^{-1} that acted as a simulacrum of a hair bundle. For a given constant force and load stiffness, the steady-state position *X* of the model bundle should accord with that of a Hookean material (Eq. **11**). The displacements of the test fiber (black circles) in response to forces delivered by a stimulus fiber are shown as a function of the added stiffness. For five levels of constant force, the application of a range of load stiffnesses yielded results demonstrating control of these parameters. The purple curves represent fits to Eq. **11**. (*B*) To test the clamp's capability to hold a hair bundle at an operating point (F_C = 0 pN; K_{EFF} = 150 and 175 μN·m^{-1}) while stimulating a hair bundle sinusoidally, we delivered time-varying stimuli to another test fiber of stiffness K_{SF} = 109 μN·m^{-1} and damping coefficient ξ_{SF} = 133 nN·s·m^{-1}. Stimulation at different frequencies yielded a response (black) that closely resembled the commanded signal (red). (*C*) The ratio of the amplitude of the fiber's motion to the amplitude of the command signal deviates from the ideal by less than 2% at all frequencies at a gain of 0.3 (cyan) or 0.46 (purple). (*D*) The fiber's displacement lags the stimulus force to a small extent at all frequencies, increasing to 16° at 100 Hz. This dependence of phase on frequency is the same for a gain of 0.3 (cyan) or 0.46 (purple).

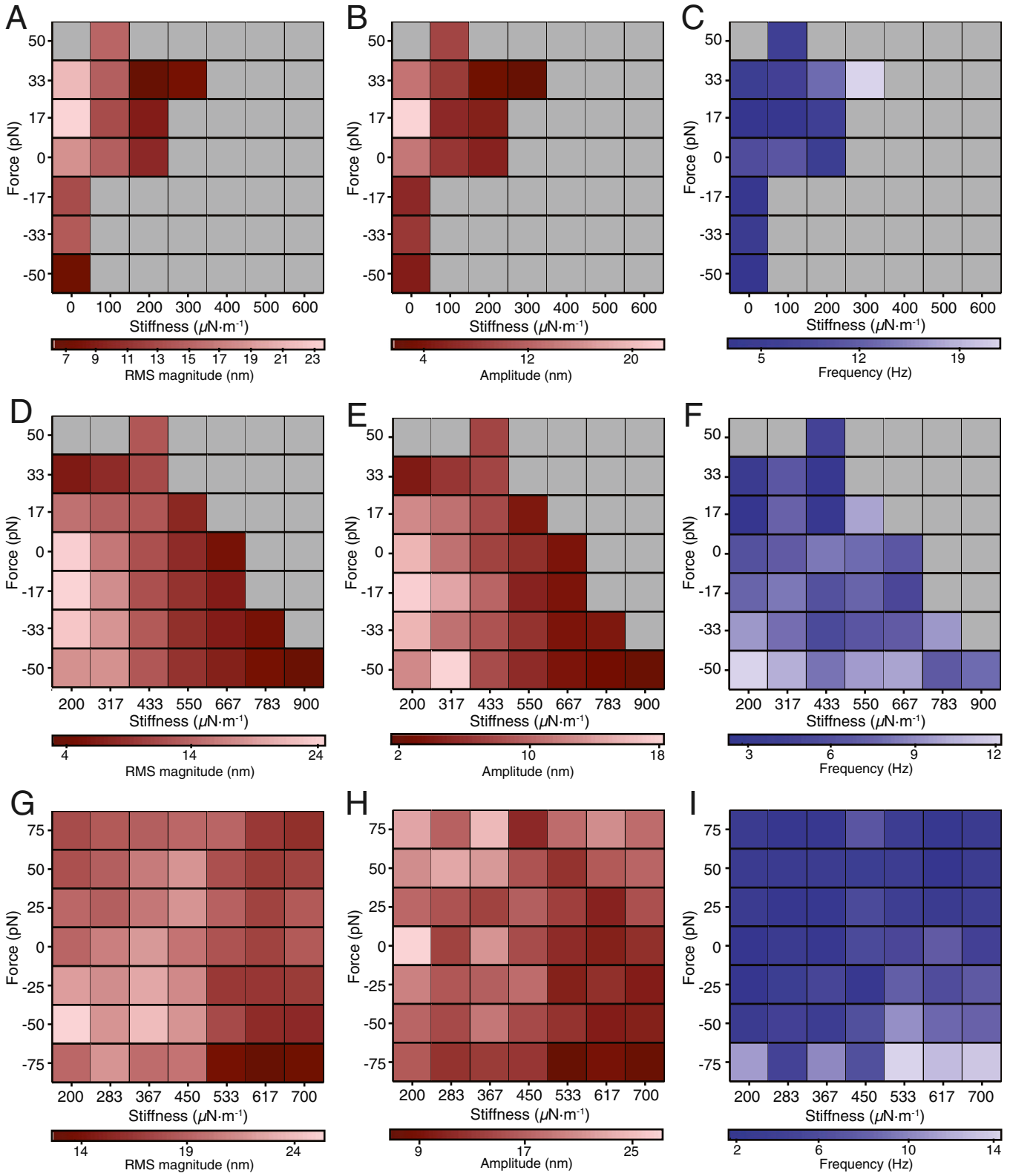

Fig. S2. Additional hair-bundle experimental state diagrams. We produced detailed experimental state diagrams for three hair bundles in addition to those analyzed in Fig. 2. In the experimental state diagrams computed for two medium hair bundles (*A–C, D–F*) and one large hair bundle (*G–I*), all quiescent operating points are displayed in gray. For oscillatory operating points, the shades of red correspond to either the RMS magnitude or the amplitude of spontaneous oscillation. The shades of blue indicate the frequency of spontaneous oscillations. For both medium bundles, we encountered a border along which oscillations were suppressed. Near the border, the peak frequencies were (*C*) 20 and (*F*) 10 Hz. In the case of the large bundle, we were unable to suppress spontaneous oscillations. In many instances the amplitude was inversely correlated with the oscillation frequency (Table S1). The peak frequencies of spontaneous oscillations in these cells accorded with the range of characteristic frequencies for afferent nerve fibers from the bullfrog's sacculus.

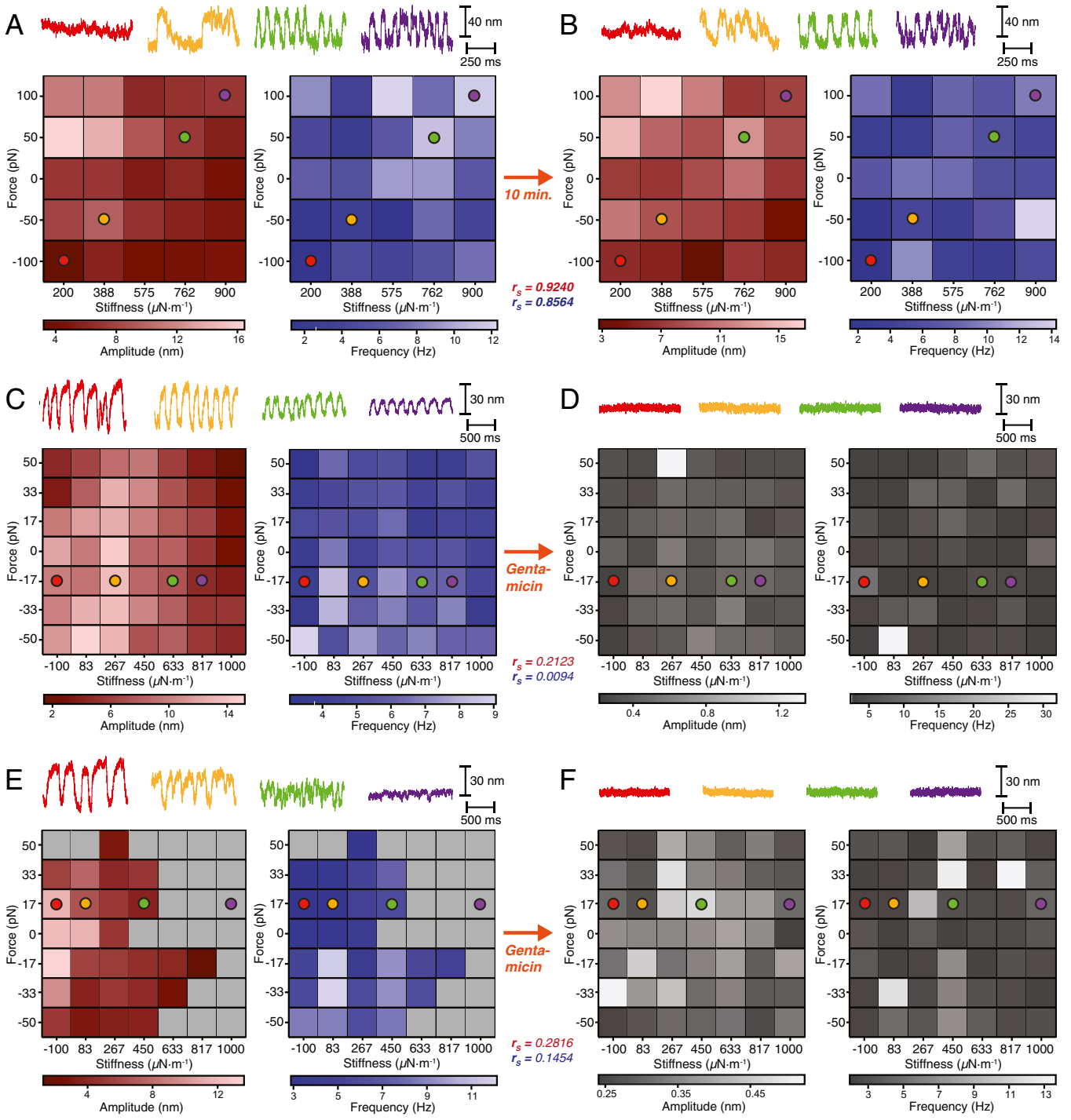

Fig. S3. State-diagram controls. (*A* and *B*) As expected for an in vitro preparation, the activity of a hair bundle deteriorates gradually during protracted recording. If a hair cell were to exhibit significant changes in its state diagram over the course of an experiment, our conclusions would be compromised. To determine whether the results remained consistent over time, we computed a bundle's experimental state diagram at two times separated by 10 min. Contrary to the general practice, we did not exchange the artificial endolymph every 4–6 min. The shades of red and blue correspond to respectively the amplitude and frequency of spontaneous oscillation. The data reveal little change in the bundle's state space over the course of the experiment, with correlation coefficients between the two diagrams of 0.92 ($P < 10^{-15}$) for amplitude and 0.86 ($P < 10^{-10}$) for frequency. (*C*–*F*) To better grasp the contribution of active hair-bundle motility on the bundle's state space, we computed the experimental state diagrams of two bundles bathed in 500 μM gentamicin, which blocks mechano-transduction channels and arrests spontaneous oscillations. (*C*) Experimental state diagrams were first constructed for a large hair bundle under control conditions. The oscillations had a maximal RMS magnitude of 16 nm and a mean of 8.7 nm. (*D*) During exposure to gentamicin the bundle became quiescent at all operating points. The amplitude map shows consistently small amplitudes, with a maximum RMS magnitude of 2.0 nm and a mean of 1.4 nm. The correlation between the state diagrams before and after treatment was not significant, with coefficients of 0.21 ($P = 0.14$) for amplitude and 0.01 ($P = 0.95$) for frequency. (*E*) Experimental state diagrams were constructed for a medium hair bundle that oscillated for about half of the operating points. The greatest RMS magnitude was of 15.6 nm and the mean RMS magnitude was 4.5 nm. (*F*) Upon exposure to gentamicin the bundle became quiescent at all operating points, with a maximal RMS magnitude of 1.6 nm and a mean of 1.4 nm. As before, there was no significant correlation between the state diagrams, with coefficients

Legend continued on following page

of 0.28 ($P = 0.13$) for amplitude and 0.15 ($P = 0.32$) for frequency. In all cases, the state diagrams before and after gentamicin treatment showed no significant positive correlations. These controls verify that a hair bundle without active motility possesses no oscillatory operating points and that its experimental state diagram changes dramatically when active motility is abolished. The analysis and parameter values for these experiments may be found in Table S1.

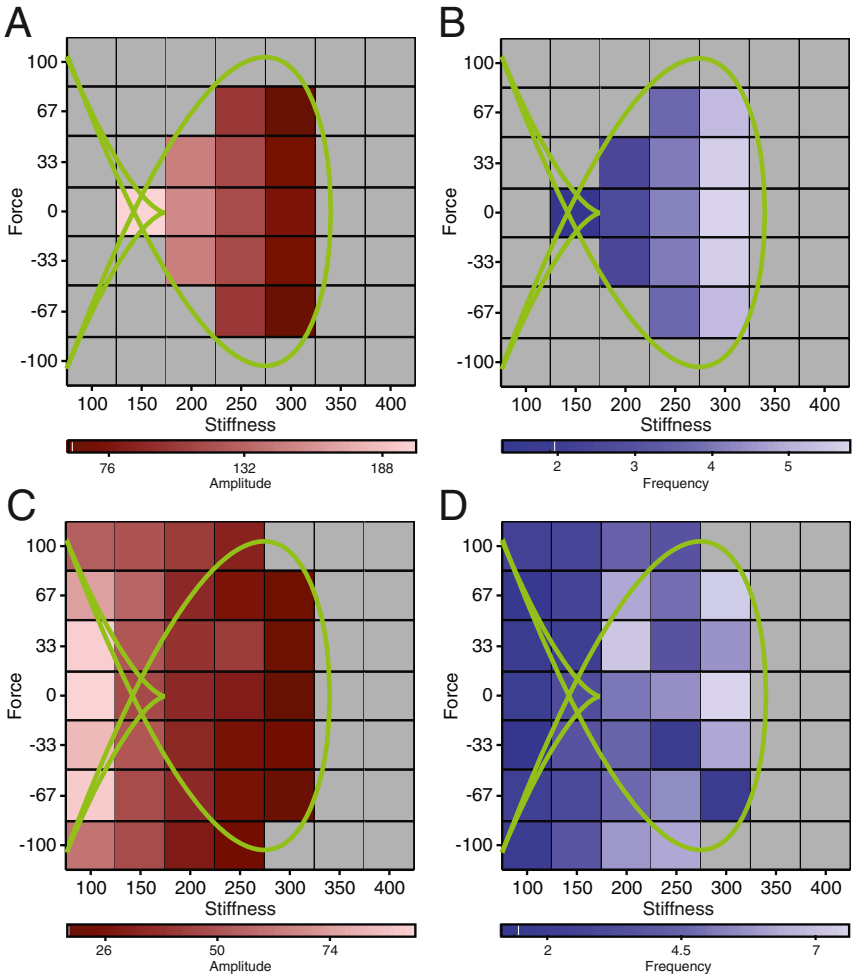

Fig. S4. Artificial state diagrams with noise. (*A*) An artificial state diagram was generated in a model of hair-bundle mechanics with a low noise level: the SDs of the noise terms were $\sigma_x = 0.001$ and $\sigma_f = 0.001$. The green lines correspond to a loop of Hopf bifurcations and a line of fold bifurcations. The gray operating points were classified as quiescent. Within the red region of spontaneous oscillation, color intensity corresponds to the amplitude of spontaneous oscillation. The smallest amplitudes were found near the high-stiffness border of the oscillatory region. (*B*) A second artificial state diagram under the same conditions depicts the oscillation frequency in blue. Near the edge of the region of spontaneous oscillation, frequencies reached their maximum. (*C*) Another artificial state diagram was generated with a high noise level: the SDs of the noise terms were $\sigma_x = 1$ and $\sigma_f = 1$. As before, the amplitude of spontaneous oscillation is displayed in red and quiescent operating points are presented in gray. In this case, the region of spontaneous oscillation increased in size. (*D*) For the same noise level, an artificial state diagram presents the frequency of spontaneous oscillation in blue. As for the previous simulation, the amplitude and frequency of spontaneous oscillation were inversely correlated, with the minimum amplitude and maximum frequency both occurring near the high-stiffness edge of the oscillatory region. The constant force, stiffness, displacement, and frequency have been rescaled by a factor of 100. Because the model incorporates rescaled parameters, no units for the amplitude, constant force, and load stiffness are displayed. All simulation results used the same values of *a, b,* and τ as the original description of the theoretical model (1). The analysis parameters and correlation statistics may be found in Table S1.

1. Ó Maoiléidigh D, Nicola EM, Hudspeth AJ (2012) The diverse effects of mechanical loading on active hair bundles. *Proc Natl Acad Sci USA* 109(6):1943–1948.

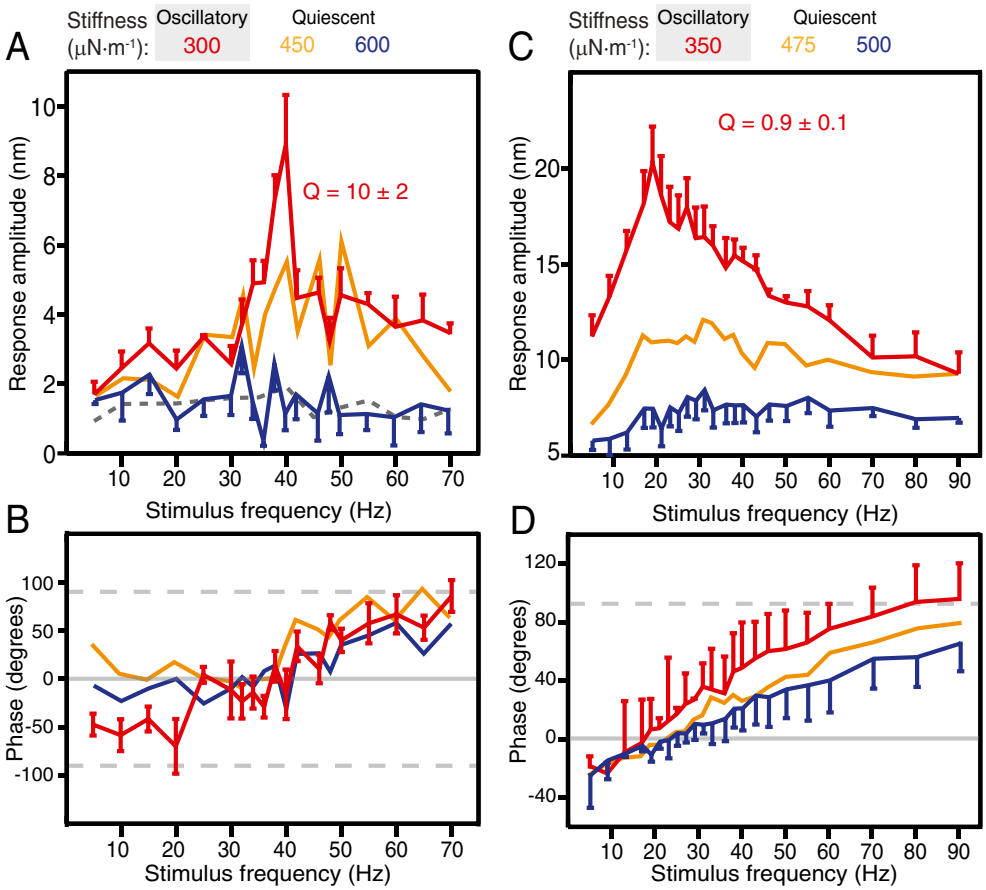

Fig. S5. Additional examples of active hair-bundle resonance. (*A* and *C*) The behavior of two hair bundles was first classified for different operating points in the absence of stimulation. The hair bundle's amplitude of vibration in response to sinusoidal stimulation was then analyzed as a function of the stimulus frequency. The responses peaked at 40 (*A*) and 20 Hz (*C*). The largest and sharpest responses occurred for operating points near the boundary of the oscillatory region. (*A*) When the bundle was exposed to 500 μM gentamicin, the frequency response lost its peak for a load stiffness of 300 $\mu N \cdot m^{-1}$ (gray dashed line). (*B* and *D*) The phase difference between the bundle's motion and that of the stimulus was calculated. A reversal from a phase lead to a phase lag occurred near the bundle's resonant frequency. This magnitude of the phase change associated with a reversal diminished upon increasing the load stiffness of the hair bundle, which moved its operating point farther from the edge of the oscillatory region.

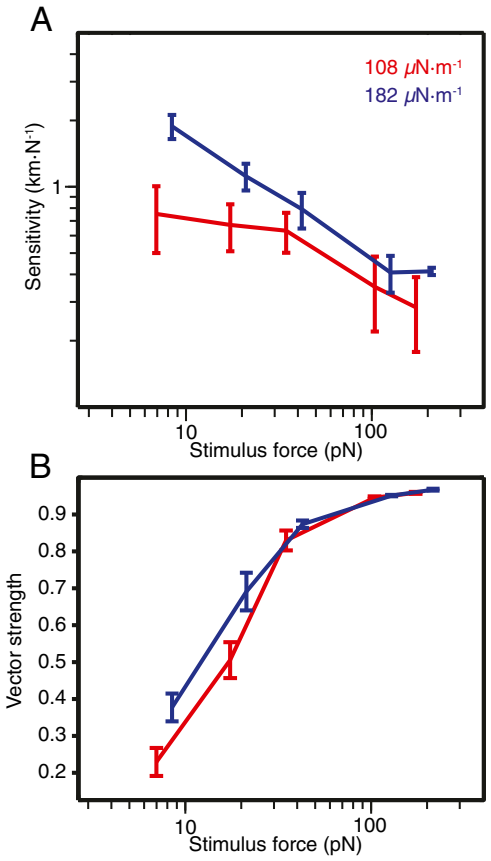

Fig. S6. Additional examples of hair-bundle sensitivity. (*A*) Stimuli of increasing magnitudes were delivered at frequencies near those of spontaneous oscillations to a hair bundle poised near the edge of its oscillatory region. The bundle's load stiffness was decreased to coax its operating point farther into the oscillatory region. (*B*) For each operating point, entrainment to stimuli was quantified by vector strength. As the force rose, the vector strength and thus the hair-bundle entrainment increased.

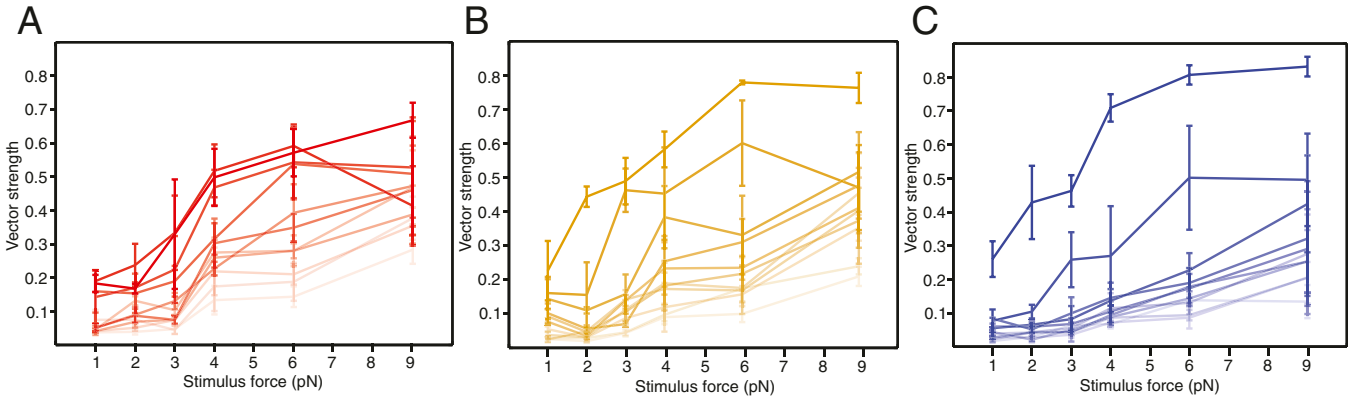

Fig. S7. Hair-bundle entrainment as a function of stimulus force across stimulus frequencies. To further assess the degree of phase locking between a hair bundle and its stimulus, we held a hair bundle at load stiffnesses of (*A*) 100, (*B*) 167, and (*C*) 250 $\mu N \cdot m^{-1}$ corresponding to operating points deep within its oscillatory region. The bundle exhibited relaxation oscillations of large amplitude and low frequency. We delivered stimuli of successively increasing forces at frequencies of 5, 9, 13, 17, 21, 24, 27, 30, 40, 60, and 80 Hz (dark to light). The degree of entrainment between the hair bundle's motion and that of the stimulus fiber is represented by the vector strength. A hair bundle achieved maximum phase locking for small forces at a stimulus frequency of 5 Hz.

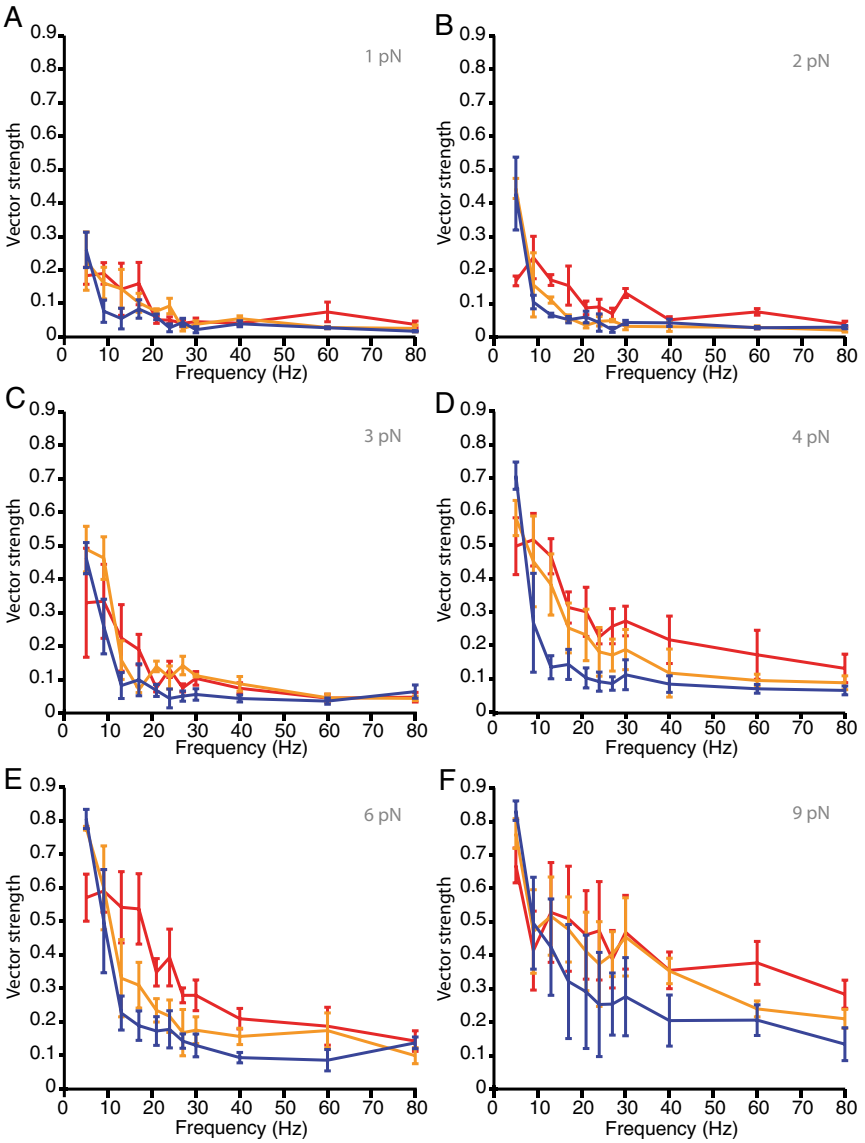

Fig. S8. Hair-bundle entrainment as a function of stimulus frequency for different stimulus forces. A hair bundle oscillated at load stiffnesses of 100 (red), 167 (yellow), and 250 $\mu N \cdot m^{-1}$ (blue). Sinusoidal forces were then delivered at amplitudes of (*A*) 1, (*B*) 2, (*C*) 3, (*D*) 4, (*E*) 6, and (*F*) 9 pN. The degree of entrainment between the stimulus fiber's motion and that of the hair bundle is represented by the vector strength (Eq. **17**). For all stimulus forces, a hair bundle achieved maximum phase locking at a stimulus frequency of 5 Hz, near its frequency of spontaneous oscillation.

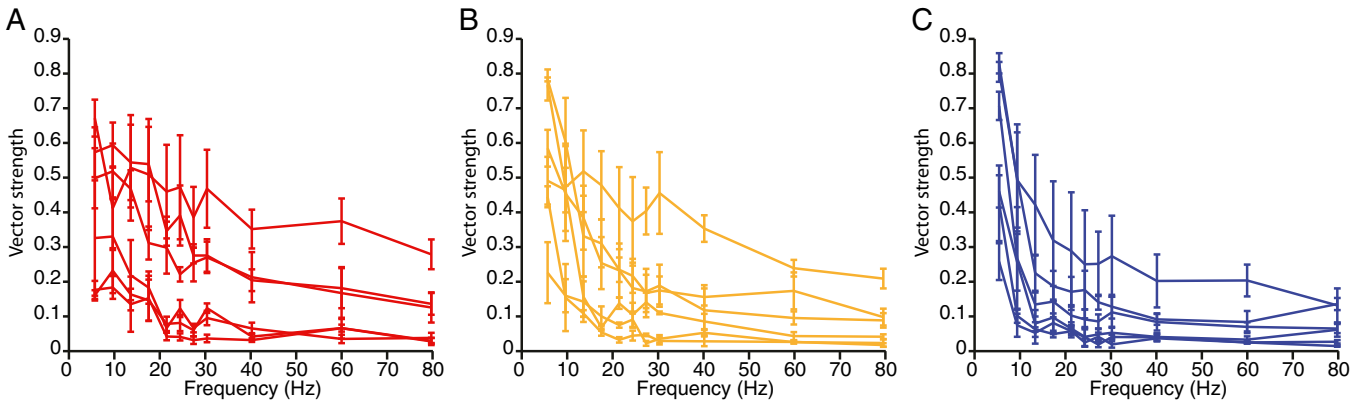

Fig. S9. Hair-bundle entrainment as a function of stimulus frequency for different operating points. A hair bundle oscillated at load stiffnesses of (*A*) 100, (*B*) 167, and (*C*) 250 $\mu N \cdot m^{-1}$. Successively increasing stimulus forces were then delivered at frequencies of 5, 9, 13, 17, 21, 24, 27, 30, 40, 60, and 80 Hz. The degree of entrainment between the hair bundle's motion and that of the stimulus fiber is represented by the vector strength. For all stimulus forces, a bundle achieved maximum phase locking at a stimulus frequency of 5 Hz. The sharpness of the relation between vector strength and stimulus frequency peaked at 250 $\mu N \cdot m^{-1}$. These data support the hypothesis that a hair bundle achieves optimal phase locking near the edge of the oscillatory region for small forcing and for small differences between the frequency of stimulation and that of spontaneous oscillation.

Table S1. Summary of state-diagram analysis and statistics

Figure	2 *A–D*	2 *E–H*	S2 *A–C*	S2 *D–F*	S2 *H–I*	2 *I–L*	S3*A*	S3*B*	S3*C*	S3*E*	S4 *A*, *B*	S4 *C*, *D*
Bundle size	Small	Medium	Medium	Medium	Large	Large	Large	Large	Large	Medium	N/A	N/A
Analysis parameters												
Detrending time (s)	2/3	1/3	1/6	1/3	1/3	1/3	2/3	2/3	2/3	2/3	0	0
Multimodality > *	1.0×10^{-3}	1.0×10^{-3}	2.0×10^{-3}	1.0×10^{-3}	1.0×10^{-2}	5.0×10^{-3}	2.0×10^{-3}	2.0×10^{-3}	1.5×10^{-2}	6.0×10^{-3}	1.0×10^{-2}	1.0×10^{-2}
Asymmetry > **	8.0×10^{-2}	5.0×10^{-2}	5.0×10^{-2}	6.0×10^{-2}	-	-	2.0×10^{-2}	2.0×10^{-2}	6.0×10^{-2}	1.3×10^{-1}	-	1.0×10^{-1}
Thinness < **	-1.8×10^{1}	-	-2.0×10^{1}	-	-	-	-1.8×10^{1}	-1.8×10^{1}	-1.8×10^{1}	-2.8×10^{1}	-	-6.0×10^{1}
Minimum Fourier frequency (Hz)	1	2	2	2	0	2	1	1	2	2	0	0
Correlations												
RMS magnitude vs. stiffness	**-4.0×10^{-1}**	**-5.4×10^{-1}**	**-5.7×10^{-1}**	**-8.1×10^{-1}**	**-6.6×10^{-1}**	**-8.0×10^{-1}**	-2.1×10^{-1}	-3.3×10^{-1}	**-7.8×10^{-1}**	**-6.9×10^{-1}**	**-9.5×10^{-1}**	**-9.7×10^{-1}**
P value	**1.7×10^{-2}**	**1.4×10^{-4}**	**3.2×10^{-2}**	**2.7×10^{-8}**	**2.9×10^{-7}**	**7.7×10^{-12}**	3.1×10^{-1}	1.1×10^{-1}	**4.5×10^{-11}**	**6.7×10^{-5}**	**1.9×10^{-7}**	**4.6×10^{-20}**
Amplitude vs. stiffness	**-4.2×10^{-1}**	**-6.2×10^{-1}**	**-6.6×10^{-1}**	**-8.6×10^{-1}**	**-5.5×10^{-1}**	**-7.7×10^{-1}**	**-4.9×10^{-1}**	-3.6×10^{-1}	**-6.6×10^{-1}**	**-7.3×10^{-1}**	**-9.5×10^{-1}**	**-9.6×10^{-1}**
P value	**1.1×10^{-2}**	**6.5×10^{-6}**	**1.1×10^{-2}**	**4.5×10^{-10}**	**3.9×10^{-5}**	**7.8×10^{-11}**	**1.2×10^{-2}**	7.3×10^{-2}	**2.1×10^{-7}**	**1.7×10^{-5}**	**1.9×10^{-7}**	**4.8×10^{-18}**
Frequency vs. stiffness	1.5×10^{-1}	**5.1×10^{-1}**	**6.0×10^{-1}**	1.0×10^{-1}	**4.1×10^{-1}**	**7.1×10^{-1}**	**4.8×10^{-1}**	2.7×10^{-1}	-3.1×10^{-2}	3.0×10^{-1}	**9.5×10^{-1}**	**6.8×10^{-1}**
P value	4.0×10^{-1}	**4.6×10^{-4}**	**2.2×10^{-2}**	6.1×10^{-1}	**3.3×10^{-3}**	**9.3×10^{-9}**	**1.5×10^{-2}**	1.8×10^{-1}	7.9×10^{-1}	1.2×10^{-1}	**1.1×10^{-7}**	**1.5×10^{-5}**
RMS magnitude vs. force	1.3×10^{-2}	**-3.7×10^{-1}**	1.7×10^{-1}	4.2×10^{-2}	-8.7×10^{-2}	-2.4×10^{-1}	**8.1×10^{-1}**	**8.3×10^{-1}**	-2.2×10^{-1}	8.2×10^{-2}	-1.2×10^{-2}	2.9×10^{-2}
P value	9.4×10^{-1}	**1.5×10^{-2}**	5.6×10^{-1}	8.2×10^{-1}	5.5×10^{-1}	9.5×10^{-2}	**8.4×10^{-7}**	**2.6×10^{-7}**	1.3×10^{-1}	6.8×10^{-1}	9.6×10^{-1}	8.7×10^{-1}
Amplitude vs. force	**3.7×10^{-1}**	**-4.4×10^{-1}**	8.1×10^{-2}	1.0×10^{-1}	**5.1×10^{-1}**	-1.5×10^{-2}	**6.2×10^{-1}**	**6.6×10^{-1}**	**-2.8×10^{-1}**	2.7×10^{-1}	-1.6×10^{-2}	1.2×10^{-1}
P value	**2.9×10^{-2}**	**3.1×10^{-3}**	7.8×10^{-1}	5.8×10^{-1}	**1.8×10^{-4}**	3.0×10^{-1}	**8.7×10^{-4}**	**3.1×10^{-4}**	**4.8×10^{-2}**	1.7×10^{-1}	9.6×10^{-1}	5.2×10^{-1}
Frequency vs. force	**-4.7×10^{-1}**	1.5×10^{-1}	5.0×10^{-1}	**-6.0×10^{-1}**	**-6.3×10^{-1}**	-2.4×10^{-1}	**4.8×10^{-1}**	2.5×10^{-1}	**-4.8×10^{-1}**	**-6.8×10^{-1}**	1.6×10^{-2}	6.8×10^{-3}
P value	**4.4×10^{-3}**	9.2×10^{-1}	7.2×10^{-2}	**3.2×10^{-4}**	**1.6×10^{-6}**	1.0×10^{-1}	**1.6×10^{-2}**	2.3×10^{-1}	**5.0×10^{-4}**	**9.8×10^{-5}**	9.6×10^{-1}	9.7×10^{-1}
Amplitude vs. frequency	**-5.7×10^{-1}**	**-6.1×10^{-1}**	-2.1×10^{-1}	3.4×10^{-2}	**-7.5×10^{-1}**	**-4.5×10^{-1}**	-5.8×10^{-2}	-2.1×10^{-1}	2.6×10^{-1}	**-4.2×10^{-1}**	**-8.2×10^{-1}**	**-7.0×10^{-1}**
P value	**3.6×10^{-4}**	**2.0×10^{-5}**	4.6×10^{-1}	8.6×10^{-1}	**6.6×10^{-10}**	**1.2×10^{-3}**	7.8×10^{-1}	3.3×10^{-1}	7.4×10^{-2}	**3.0×10^{-2}**	**3.4×10^{-4}**	**1.2×10^{-5}**

Statistics are displayed for each of the state diagrams in Fig. 2 and Figs. S2–S4. The columns corresponding to Fig. S3 depict the statistics for one hair bundle over the course of 10 min (Fig. S3 *A* and *B*) and two bundles before gentamicin treatment (Fig. S3 *C* and *E*). For each hair bundle, its size classification and analysis parameters are presented. Entries with dashed lines correspond to tests that were not required for that particular bundle. For each statistic, a threshold was placed both upon the value presented and its corresponding *P* value (*$P < 0.01$; **$P < 0.001$). Spearman's rank correlation between the bundle's RMS magnitude, amplitude, and frequency of spontaneous oscillations was calculated for each bundle with respect to both the load stiffness and constant force and between the amplitude and frequency of oscillation. Numbers in bold correspond to significant correlations ($P < 0.05$). In all cases but one, a bundle's oscillatory amplitude decreased with increasing load stiffness. For half of the bundles the frequency of oscillation grew with increasing load stiffness. In half of the instances the amplitude and frequency of spontaneous oscillation were inversely correlated.